



Research article

Unraveling the signaling network between dysregulated microRNA and mRNA expression in sevoflurane-induced developmental neurotoxicity in rat

Yuanyuan Wang^a, Xin Men^b, Xiaodong Huang^b, Xiaoxiao Qiu^b, Weilong Wang^b, Jin Zhou^b, Zhenfeng Zhou^{b,*}

^a Department of Endocrinology, Xixi Hospital of Hangzhou (Affiliated Hangzhou Xixi Hospital of Zhejiang Chinese Medical University), Hangzhou, China

^b Department of Anesthesiology, Hangzhou Women's Hospital (Hangzhou Maternity and Child Health Care Hospital, Hangzhou First People's Hospital Qianjiang New City Campus, Zhejiang Chinese Medical University), Hangzhou, China

ARTICLE INFO

Keywords:

Sevoflurane
Neurotoxicity
miRNA-mRNA network
Neuroapoptosis

ABSTRACT

Research has indicated that general anesthesia may cause neuroapoptosis and long-term cognitive dysfunction in developing animals, however, the precise mechanisms orchestrating these outcomes remain inadequately elucidated within scholarly discourse. The purpose of this study was to investigate the impact of sevoflurane on the hippocampus of developing rats by analyzing the changes in microRNA and mRNA and their interactions. Rats were exposed to sevoflurane for 4 h on their seventh day after birth, and the hippocampus was collected for analysis of neuroapoptosis by Western blot and immunohistochemistry. High-throughput sequencing was conducted to analyze the variances in miRNA and mRNA expression levels, and the Morris water maze was employed to assess long-term memory in rats exposed to sevoflurane after 8 weeks. The results showed that sevoflurane exposure led to dysregulation of 5 miRNAs and 306 mRNAs in the hippocampus. Bioinformatic analysis revealed that these dysregulated miRNA-mRNA target pairs were associated with pathological neurodevelopment and developmental disorders, such as regulation of axonogenesis, regulation of neuron projection development, regulation of neuron differentiation, transmission of nerve impulse, and neuronal cell body. Further analysis showed that these miRNAs formed potential network interactions with 44 mRNAs, and two important nodes were identified, miR-130b-5p and miR-449c-5p. Overall, this study suggests that the dysregulation of the miRNA-mRNA signaling network induced by sevoflurane may contribute to neurodevelopmental toxicity in the hippocampus of rats and be associated with long-term cognitive dysfunction.

1. Introduction

An increasing amount of evidence suggests that various anesthetics agents may have deleterious impacts on developing neural cells, thereby leading to persistent cognitive impairment [1,2]. The phenomenon of anesthetic-induced developmental neurotoxicity encompasses a spectrum of pathological events, including neuronal apoptosis, neurodegenerative processes, changes in neurogenesis and

* Corresponding author. Hangzhou Women's Hospital, No.369 Kungpeng Road, Hangzhou, Zhejiang, 310018, China.
E-mail address: zhenfeng9853@163.com (Z. Zhou).

<https://doi.org/10.1016/j.heliyon.2024.e33333>

Received 12 November 2023; Received in revised form 5 June 2024; Accepted 19 June 2024

Available online 20 June 2024

2405-8440/© 2024 The Authors. Published by Elsevier Ltd. This is an open access article under the CC BY-NC-ND license (<http://creativecommons.org/licenses/by-nc-nd/4.0/>).

synaptogenesis, as well as damage to brain circuits [3]. Sevoflurane is an inhaled anesthetic, and is widely used for both adult and pediatric patients in clinical practice due to its desirable properties, such as lack of pungent odor, low blood-gas partition coefficient, rapid onset and offset, and limited cardiopulmonary depression. However, some studies suggest that sevoflurane may have deleterious impacts on developing nervous system, particularly in infants and young children [4]. This toxicity could potentially affect the cognitive and behavioral development of children, which has raised concerns [5]. Nevertheless, the mechanism underlying sevoflurane-induced neurotoxicity remains incompletely understood.

MicroRNAs (miRNAs) are small (approximately 21 nucleotides), non-coding RNA molecules that are highly conserved throughout evolution and are encoded in the genomes of nearly all eukaryotes, from plants to mammals [6]. In mammals, predicted miRNAs control the activity of more than 60 % of the entire protein-coding genes and engage in the modulation of all cellular processes thus far [7]. Generally, miRNAs modulate the expression of genes through binding to partially complementary regions in the mRNA 3' UTR, and by promoting degradation or inhibiting translation of the target mRNA. Studies have shown that individual genes can be subject to regulation by multiple miRNAs, and a single miRNA can also regulate multiple mRNA targets simultaneously [8,9]. As the field of miRNA research has developed, it has become clear that miRNA function is extremely complex, with a complex network of factors strictly controlling miRNA processing and biological activity. Dysregulated miRNA expression has been found to play a critical role in various pathological processes, including neurological disorders, cardiovascular disease, cancer and viral infections [10]. The multifunctionality and potential of miRNAs make them a valuable resource for both basic research and clinical applications.

MiRNAs and their associated regulatory networks are becoming increasingly recognized for their roles in regulating complex neurobiological functions. Research has shown that the spatiotemporal expression patterns of miRNAs play crucial roles in mammalian neural development. Dysregulated miRNA/mRNA interactions can form extensive molecular networks, potentially affecting diverse neural functional pathways in the hippocampus, thereby lead to neuronal cell damage and harm long-term memory [11,12]. Numerous studies have highlighted the pivotal role of microRNAs in sevoflurane-induced developmental neurotoxicity, with specific miRNA/mRNA axes such as miR-330-3p/ULK1, lncRNA Neat1/miR-298-5p/SRPK1, lncRNA PEG13/miR-128-3p/SOX13, and Rik-203/miR-4661-3p/BDNF being implicated in the pathogenesis of sevoflurane-induced neurotoxicity during neurodevelopmental stages [13–16]. Therefore, the primary objective of this inquiry is to scrutinize the impact of sevoflurane exposure on the expression profiles of miRNAs and mRNAs in the developing rat hippocampus, employing bioinformatics methodologies to prognosticate disease pathways, delineate miRNA-mRNA interactions, and unravel pertinent cellular pathways. These endeavors aim to provide further insights into the diverse mechanisms underlying the neurotoxic effects of sevoflurane exposure during development.

2. Materials and methods

2.1. Animal studies

Approval for this investigation was obtained from the Animal Research Committee of Zhejiang Provincial People's Hospital (No. 2021082), with adherence to the "Guidelines for the Care and Use of Laboratory Animals" in all experimental procedures. All animals used in the experiment were postnatal day 7 (P7) SD rat pups from GemPharmatech (Nanjing, China). The rat pups were exposed to 3.4 % sevoflurane or only fresh gas for a duration of 4 h within a chamber (RWD Life Science) at room temperature [17]. To sustain a consistent concentration of 3.4 % sevoflurane throughout the trials, a Capnomac gas monitor (Datex-Ohmeda) was employed. After the experiment, all animals were euthanized for isolation of hippocampal tissues in accordance with the "AVMA Guidelines for the Euthanasia of Animals". This process involved placing the animals in a carbon dioxide environment for a duration of 5 min until cessation of respiration and cardiac activity was confirmed.

2.2. Western blot analysis

Hippocampal tissues underwent lysis in RIPA buffer supplemented with protease inhibitor, followed by quantification of protein concentration utilizing a BCA kit. Subsequent to lysis, the protein extracts were subjected to separation via SDS-PAGE and transferred onto a PVDF membrane. To mitigate non-specific binding, the membrane was treated with a blocking solution comprising non-fat milk, followed by incubation with primary antibodies alongside a loading control such as GAPDH. Following thorough washing steps, the membrane was exposed to HRP-conjugated secondary antibodies. Visualization and quantification of protein bands were achieved utilizing an ECL kit in conjunction with ImageJ software.

2.3. Immunohistochemistry

Immunohistochemical analysis was conducted on formalin-fixed, paraffin-embedded tissue sections. Following deparaffinization and rehydration procedures, antigen retrieval was facilitated by subjecting the sections to boiling in citrate buffer (pH 6.0) for a duration of 20 min. To mitigate endogenous peroxidase activity, treatment with 3 % H₂O₂ in methanol was administered for a duration of 15 min. Subsequently, incubation with primary antibodies targeting the proteins of interest was carried out overnight at 4 °C. Following thorough washing with PBS, the sections underwent incubation with HRP-conjugated secondary antibodies for 30 min at ambient temperature. Signal visualization was accomplished through the utilization of DAB substrate, accompanied by counterstaining with hematoxylin. Subsequent to dehydration, the slides were mounted and subjected to microscopic imaging. Negative controls were integrated by excluding the primary antibody from the staining protocol.

2.4. Morris water maze (MWM) test

Eight weeks post-exposure to sevoflurane, spatial learning and memory in rats were assessed through the Morris water maze. The maze setup included a circular pool with water rendered opaque by the addition of non-toxic white paint. A platform, 10 cm in diameter, was submerged 1 cm beneath the water surface within one of the four quadrants. Training for each rat spanned five days, during which they were taught to locate the platform using visual cues present in the room. On the sixth day, a probe trial was conducted where the platform was removed, allowing the rats to swim for 120 s. Measurements were taken of the time spent in each quadrant and the frequency of platform crossings. The test was performed blind to the experimental group.

2.5. Expression profile analysis of miRNA and mRNA

Total RNA extraction from tissue samples was carried out utilizing a commercial kit, adhering strictly to the provided protocol. The quality and quantity of the extracted RNA were evaluated with a NanoDrop spectrophotometer. The RNA was then sent to a commercial sequencing company for library preparation and sequencing. miRNA uses Bowtie-1.0.0 for read alignment and ACGT101-miR (v4.2) software for miRNA identification. Expression levels are normalized using norm values, and target gene prediction is performed using a combination of TargetScan v5.0 and Miranda v3.3 software [18]. For RNA-seq, reads of all samples were aligned to the reference genome of the research species using HISAT2 [19]. StringTie and Ballgown were used to estimate transcript expression levels and calculate FPKM values for mRNAs. The R package EdgeR was employed to process both miRNA-seq and mRNA-seq data between two conditions utilizing a negative binomial generalized linear model with a likelihood ratio test (glmLRT). To visualize the abundance of miRNAs/genes, perform heatmap clustering analysis, and investigate miRNA-mRNA correlations, the count-per-million values were converted to log₂ scale (LogCPM). The results of miRNA and mRNA expression profiling were integrated to identify potential miRNA-mRNA regulatory networks.

2.6. RT-qPCR

Total RNA was isolated from tissue samples following the manufacturer's protocol using a commercial extraction kit. The RNA's quality and concentration were determined with a NanoDrop spectrophotometer. Subsequently, cDNA was synthesized from 1 µg of total RNA utilizing a reverse transcription kit. Real-time PCR was carried out with a SYBR Green master mix and gene-specific primers. The thermal cycling parameters were set as follows: an initial denaturation at 95 °C for 10 min, then 40 cycles at 95 °C for 15 s and 60 °C for 1 min. The relative expression levels of target genes were quantified using the $2^{-\Delta\Delta Ct}$ method, with normalization to an endogenous reference gene.

2.7. Statistical analysis

Statistical analyses were conducted utilizing GraphPad Software and SPSS 24.0. Data are expressed as mean ± standard deviation. Comparisons between two groups were made using a Student's t-test, while comparisons among more than two groups were performed using a one-way analysis of variance (ANOVA) followed by Bonferroni's multiple comparison test. A P-value of less than 0.05 was deemed statistically significant. Animal allocation was randomized according to weight, and all animals were included in the study without any exclusions.

3. Result

3.1. Sevoflurane exposure has no effect on physiological conditions in rat

During sevoflurane anesthesia, all rat pups survived, and their body temperature was consistently maintained at 37 ± 0.5 °C. Additionally, arterial blood gas parameters (Table 1) showed no significant differences between the control group and the sevoflurane-exposed group, indicating that sevoflurane anesthesia did not have a significant impact on the physiological condition of the rat pups.

3.2. Sevoflurane can cause developmental neurotoxic effects

Exposure to sevoflurane for 4 h increased the expression of Bax and cleaved caspase 3 proteins, while decreasing the expression of

Table 1
Arterial blood pressure and arterial blood gas analysis.

	Time	pH	PaCO ₂ , mmHg	PaO ₂ , mmHg	SaO ₂ %	MAP, mmHg
Con (n = 6)	0 h	6.87 ± 0.03	39.4 ± 3.8	98.2 ± 6.3	99.5 ± 0.3	50 ± 4
	6 h	6.79 ± 0.04	40.3 ± 4.2	99.1 ± 7.2	99.3 ± 0.5	48 ± 3
3.4 % SEVO (n = 6)	0 h	6.82 ± 0.06	39.8 ± 5.3	98.7 ± 7.1	99.1 ± 0.4	49 ± 6
	6 h	6.78 ± 0.04	41.3 ± 4.3	99.2 ± 6.6	98.5 ± 0.6	48 ± 5

PaCO₂ = arterial carbon dioxide tension; PaO₂ = arterial oxygen tension; SaO₂ = arterial oxygen saturation.

Bcl-2 protein in the hippocampus of day 7 rat pups, indicating induction of apoptosis (Fig. 1A). The TUNEL assay was utilized to identify apoptotic cells within the hippocampal tissue samples. Following TUNEL and hematoxylin staining, apoptotic cell nuclei exhibited a brown stain, while normal nuclei appeared blue. Analysis revealed a noteworthy elevation in apoptotic cell count within the sevoflurane-exposed group compared to the control group ($P < 0.05$) (Fig. 1B). Additionally, to further investigate the impact of sevoflurane on learning and memory ability in neonatal rat, the Morris water maze (MWM) test were carried out in rat 8 weeks after Sevoflurane exposure (Fig. 1C). Our findings indicate a significant increase in swim latencies and a notable decrease in crossing numbers during the MWM in rats following sevoflurane exposure (Fig. 1D). These findings suggest that sevoflurane exposure may impair long-term memory function.

3.3. Sevoflurane exposure alters mRNA profiles in the hippocampus of rat pup

To investigate the transcriptional changes induced by sevoflurane exposure, we conducted a high-throughput RNA-sequencing (RNA-seq) analysis aiming to identify similarities and differences in gene expression profiles. Utilizing violin plot analysis and Pearson's correlation, we observed that intergroup correlations between sevoflurane and control mRNA expression profile on Day 7 rats were high similarity (Fig. 2A and B). Out of the 28,970 mRNA transcripts that were analyzed, 306 were found to be dysregulated (168 upregulated and 138 downregulated) in the hippocampi of rats exposed to sevoflurane at Day 7 ($|\log_{2}FC| > 2$, $P < 0.05$). The volcano plot depicted the differential abundance of mRNAs within the hippocampi between the control and sevoflurane groups (Fig. 2C, Table S1). Furthermore, heatmaps were created using the most significant differentially expressed genes in each group, revealing a notably distinct pattern associated with sevoflurane exposure in contrast to the control group (Fig. 2D).

3.4. GO and KEGG pathway analysis screen sevoflurane-associated signal pathways

We combined RNA-seq with GO and KEGG pathway analyses to identify the signal pathways enriched by Sevoflurane treatment. Differential gene expression analysis was conducted using GO and KEGG pathway analyses. GO analysis included three subtypes: biological process (BP), cellular component (CC), and molecular function (MF). Among the differentially expressed genes, Sevoflurane treatment was found to be associated with oxygen binding, oxygen carrier activity, oxygen transport, lipoxygenase pathway, hemoglobin complex, extracellular matrix, and other related functions (Fig. 3A–C). Additionally, KEGG serves as a database connecting genomic information with higher-order functional information. Specifically, the differentially expressed genes associated with sevoflurane treatment in hippocampal cells were found to be involved in cytokine-cytokine receptor interaction, metabolic pathways, neuroactive ligand-receptor interaction, human papillomavirus infection, and others (Fig. 3D).

3.5. Potential signaling pathways for sevoflurane dysregulated miRNA in the hippocampus of rat pup

To identify differentially expressed miRNAs between the sevoflurane-treated and control groups, miRNA sequencing was performed on hippocampal cell RNA. We identified a total of 632 miRNAs in both groups. The following criteria was performed to filter

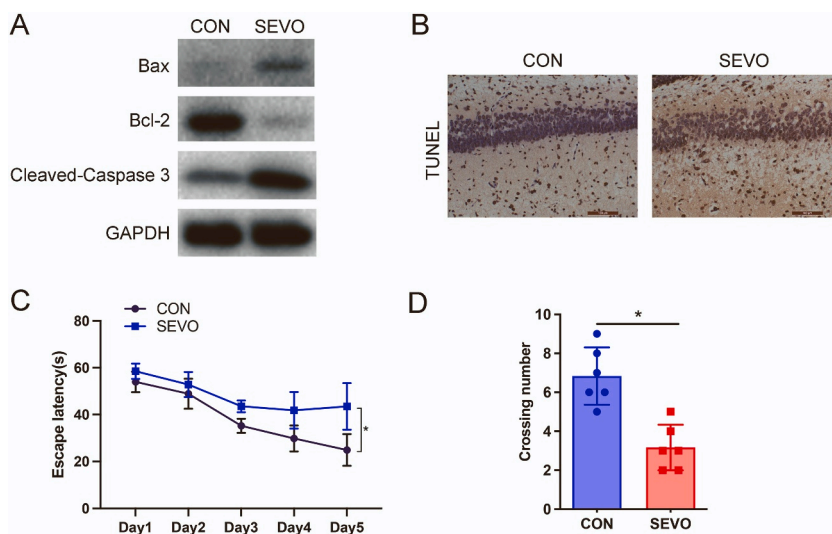


Fig. 1. Sevoflurane exposure causes hippocampal cell apoptosis and impairs long-term memory in rat pups. (A) Apoptosis in the hippocampus of rats was evaluated by detecting the expression of apoptosis-related proteins Bax, Bcl-2, and cleaved caspase 3 using Western blotting. The unedited images are referenced in Fig. S2 (B) TUNEL staining was used to identify cell apoptosis by immunohistochemistry. (C) The escape latencies were measured over five consecutive training days to assess learning and memory in the two groups. (D) The average number of crossings over the platform-site during the probe trial was calculated as an indicator of spatial memory.

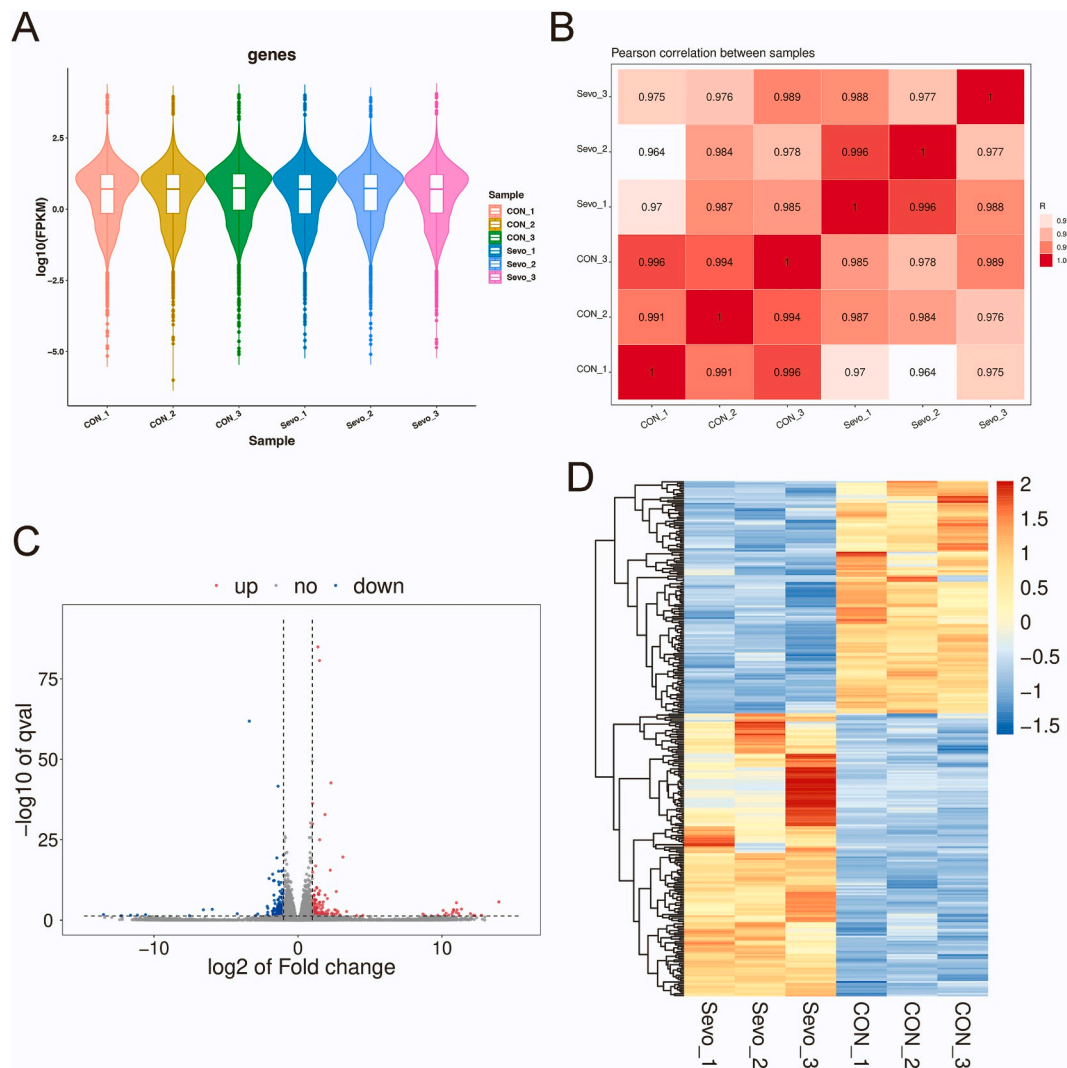


Fig. 2. Sevoflurane induces differential mRNA expression profiles in the hippocampus of rats. (A, B) Violin plots and Pearson correlation coefficients heatmap show the similar distribution of normalized mRNA signal intensities in the hippocampus of six rats. (C) The volcano plot displays the differentially expressed mRNAs between the control and sevoflurane groups. Red dots indicate upregulated mRNAs, while blue dots indicate downregulated mRNAs, with $p < 0.05$ and fold change ≥ 2 compared to the control. (D) The heatmap clustering analysis shows the expression profiles of differentially expressed mRNAs induced by sevoflurane in the hippocampus of rats ($p < 0.05$). Each row represents the relative expression level of an mRNA gene. (For interpretation of the references to colour in this figure legend, the reader is referred to the Web version of this article.)

the significant miRNAs: P -value < 0.05 and fold change > 1.0 (or < 1.0). Five significantly differentially expressed miRNAs were identified in the volcano plot (rno-miR-449a-3p, rno-miR-449c-5p, rno-miR-652-5p, rno-miR-130b-5p, rno-miR-451-5p) (Fig. 4A and Table S1). In addition, hierarchical clustering of these miRNAs depicted 36 upregulated and 38 downregulated miRNAs (Fig. 4B). Subsequent analyses included differential expression miRNA target prediction, GO enrichment, and KEGG pathway assessments. A total of 2453 target genes were identified for the 5 differentially expressed miRNAs through TargetScan and miRanda. These target genes were predominantly associated with synaptic membrane, regulation of neuron differentiation, regulation of neuron projection development, regulation of axonogenesis, transmission of nerve impulse, and neuronal cell body (Fig. 4C–E). Enriched pathways included MAPK signaling pathway, Neurotrophin signaling pathway, PI3K-Akt signaling pathway and Wnt signaling pathway (Fig. 4F).

3.6. Sevoflurane-induced dysregulation of miRNA-mRNA interaction network

Studies have shown that miRNA can bind to target mRNA and exert negative regulation by complementary interaction through its seed sequence, thereby reducing the expression level of the target mRNA or inhibiting its translation process. In order to identify potential mRNA targets of dysregulated miRNAs and potential signaling pathways involved in sevoflurane-induced developmental

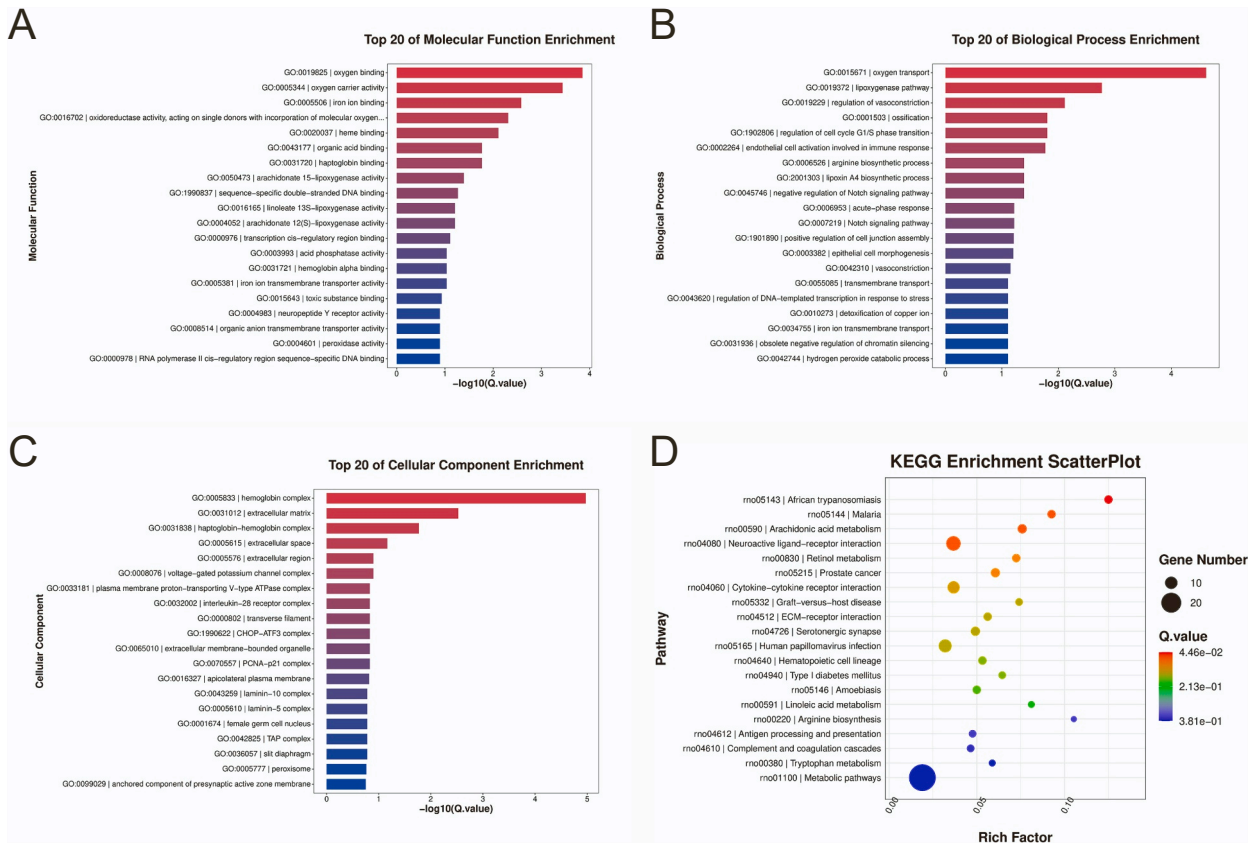


Fig. 3. GO and KEGG enrichment analysis of DEPs in the Sevo group compared to control group.(A) Molecular function of GO analysis; (B) Biological process of GO analysis; (C) Cellular component of GO analysis; (D) Scatterplot of enriched KEGG pathways.

neurotoxicity, we employed TargetScan and miRanda for the prediction of potential target genes of the 5 significantly differentially expressed miRNAs. We then cross-referenced these potential target genes with the RNA-seq data after sevoflurane treatment. The targets of miR-449c-5p, miR-652-5p, miR-451-5p, miR-449a-3p, and miR-130b-5p have 17, 4, 2, 6, and 15 genes, respectively, in the differential gene list from RNA-seq (Fig. S1). Using Cytoscape, we established a network comprising 5 miRNAs and 44 potential mRNA targets, where each connection represented a putative regulatory cascade after sevoflurane exposure in rat pups. Interestingly, miR-130b-5p and miR-449c-5p constituted two important nodes, with over 10 putative associated targets each. Certain mRNAs exhibited the potential to be targeted by two distinct miRNAs, indicating the existence of fine-tuning regulatory mechanisms (Fig. 5). The expression patterns of numerous predicted target mRNAs demonstrated an inverse correlation with the expression of their corresponding miRNAs, as indicated by red boxes in the figure, supporting the proposed miRNA-dependent regulation.

3.7. RT-qPCR validation of differential circRNA and miRNA expression

RT-qPCR validated the expression trends of miRNAs and target mRNAs under sevoflurane treatment, which were consistent with the sequencing data. To investigate the expression of miRNA and mRNA from bioinformatics analysis and determine their significance in Sevoflurane-induced neurotoxicity, we used RT-qPCR to confirm the expression of some miRNA and mRNA in newly processed Sevoflurane-exposed and control groups. RT-qPCR was employed to assess the variance in expression levels of 5 miRNAs and 13 mRNAs between the Sevoflurane group (n = 10) and the control group (n = 10). Findings revealed a significant upregulation of miR-130b-5p and miR-449c-5p in the Sevoflurane group (Fig. 6A, P < 0.05); the target genes of miR-449c-5p, Gnrhr and Abcc6, were significantly downregulated (Fig. 6B, P < 0.05); and the target genes of miR-130b-5p, Gja5, Nags, and Cyyr1, were significantly downregulated (Fig. 6C, P < 0.05). In addition, Pearson correlation between miRNA and target gene expression showed significant negative correlation between miR-130b-5p and Gja5 (P = 0.0051), as well as between miR-449c-5p and Gnrhr (P = 0.0129) (Fig. 6D). This suggests that these two pairs of miRNA-mRNA networks may be potential important targets for Sevoflurane-induced neurotoxicity.

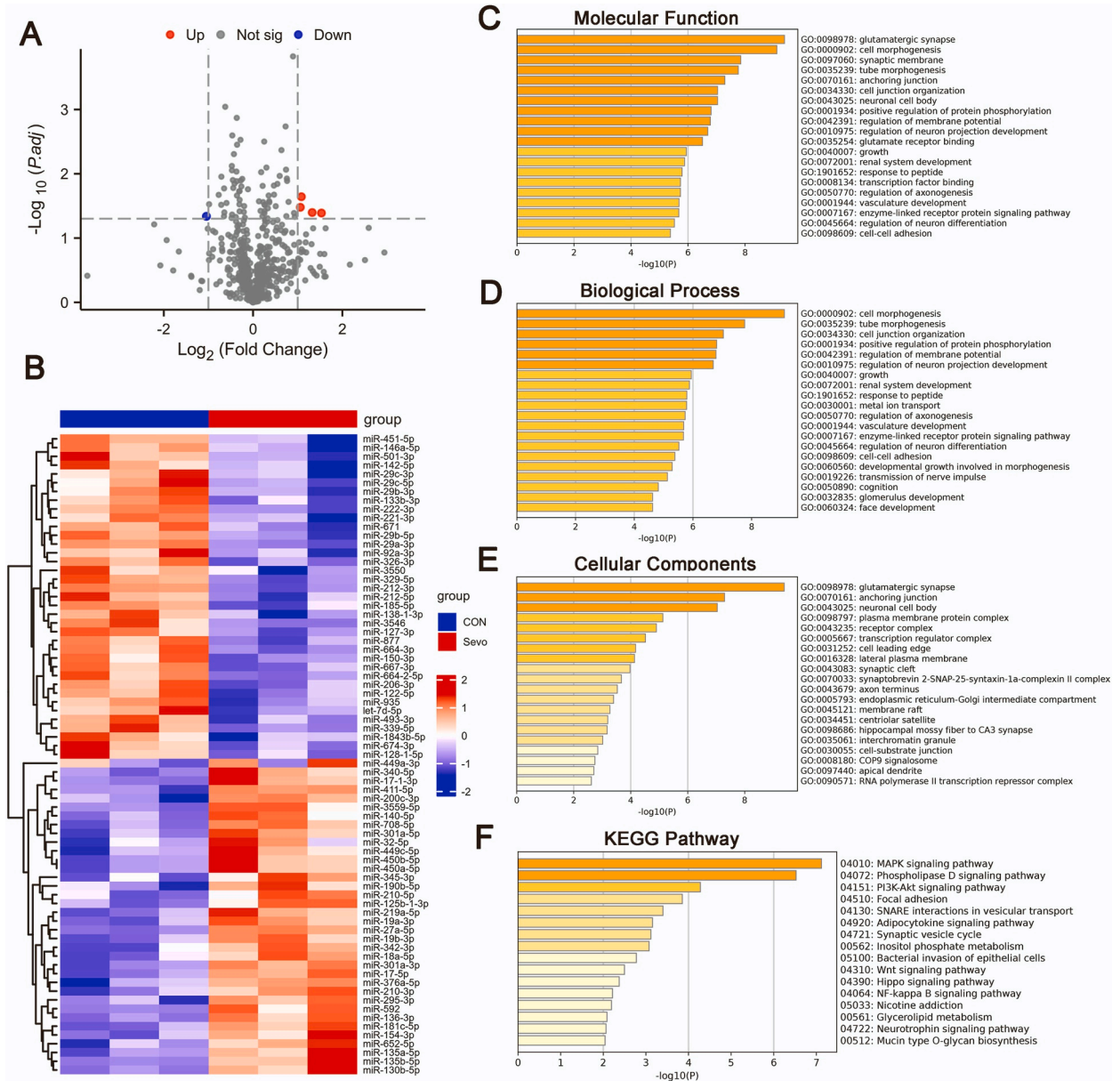


Fig. 4. Bioinformatics analysis of miRNA dysregulation induced by sevoflurane. (A) Volcano plot displays miRNAs with significant expression differences. (B) Heat map of differentially expressed miRNAs between Sevo group and control group. (C–E) GO analysis includes Molecular function, Biological process, and Cellular component. (F) KEGG pathway enrichment analysis of differentially expressed genes on miRNA-seq.

4. Discussion

This is the first study to explore the dysregulation of miRNA-mRNA expression profiles in rat hippocampal tissue induced by sevoflurane from the perspective of interactive signaling pathways. We found that sevoflurane can induce acute neurocyte apoptosis in the hippocampus of neonatal rats and impair their long-term memory ability. The acute neurotoxic effects induced by sevoflurane were concomitant with notable expression variations in 5 miRNAs and 306 mRNAs. Pathway enrichment analysis showed that the dysregulated miRNA-mRNA interactions induced by sevoflurane were involved in various pathways such as neurodevelopmental disorders and axonogenesis. Specifically, bioinformatics analysis indicated that 44 dysregulated mRNAs could potentially serve as target genes for 5 aberrantly expressed miRNAs, thereby forming several miRNA-mRNA interaction pairs. These aberrantly dysregulated miRNA-mRNA target pairs may be important factors in the pathological neurotoxic and developmental disorders induced by sevoflurane in rats.

Neuronal apoptosis stands as an extensively investigated neurodegenerative consequence subsequent to developmental sevoflurane

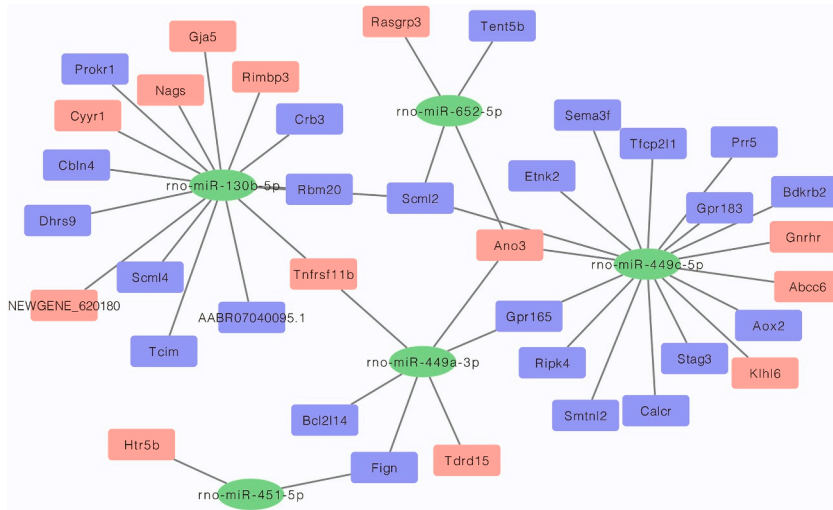


Fig. 5. Coding (mRNA) and non-coding gene (miRNA) interaction networks image based on the Cytoscape analysis of the 5 significantly expressed miRNAs and 44 candidate mRNA targets. circle node: miRNAs. square node: mRNAs. Solid line: potential interaction relationships.

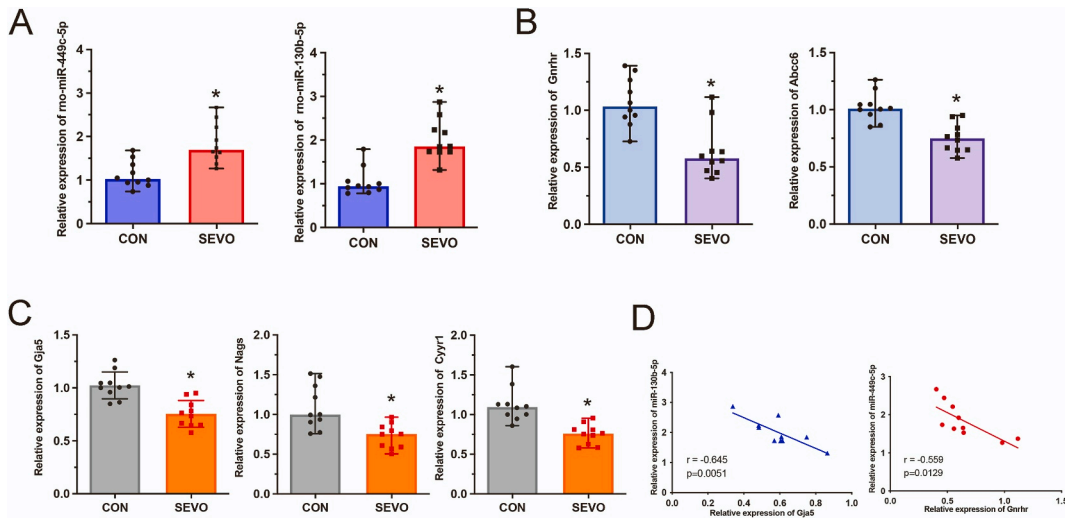


Fig. 6. RT-qPCR results showing relative levels of expression of various response genes induced by Sevoflurane. (A) The RT-qPCR confirmed that miR-130b-5p and miR-449c-5p were significantly upregulated among the five differentially expressed miRNAs. (B) The expression of Gnrhr and Abcc6, which were identified as potential targets of miR-449c-5p, was significantly reduced in the sevoflurane group. (C) The expression of Gja5, Nags, and Cyrr1, which were identified as potential targets of miR-130b-5p, was significantly reduced in the sevoflurane group. (D) Pearson correlation between miRNA and target gene expression.

exposure [20,21]. Current research has evaluated neuronal apoptosis after 4 h of sevoflurane exposure, indicating that sevoflurane-induced neuronal damage rapidly initiates early apoptosis through direct cellular or molecular events. However, the precise mechanism by which these initial apoptotic effects of sevoflurane translate into enduring cognitive impairment remains unknown. Moreover, it may require multiple molecular networks to maintain the integrity of neurons [22]. Through bioinformatics analysis of miRNA-mRNA interaction networks, our study provides many clues to this question and provides significant information for prospective mechanistic inquiries in this domain.

We focused on the impact of sevoflurane-induced changes in miRNA-mRNA expression profiles [23]. The rat miRNA-mRNA profile and pathway analysis were conducted at an early time point (4 h) after neonatal exposure to sevoflurane, as the focus was on exploring the aberrantly regulated cellular and molecular pathways during the acute phase of sevoflurane toxicity [24,25]. Sevoflurane-induced neurotoxicity represents a multifaceted physiological and pathological process, and single exposure to anesthetics during early individual development may result in long-term defects. Furthermore, the transient cellular and molecular changes triggered by sevoflurane toxicity can exert long-lasting effects on behavior and function. Moreover, just as the transient cellular and molecular changes triggered by sevoflurane toxicity can exert long-lasting effects on behavior and function, the miRNA-mRNA network and its

corresponding pathways are likely to be upregulated or downregulated at different developmental stages, which may contribute to the progression of neurotoxicity [26–28]. Based on our data, we identified 5 miRNAs (rno-miR-449a-3p, rno-miR-449c-5p, rno-miR-652-5p, rno-miR-130b-5p, rno-miR-451-5p) and 44 putative dysregulated mRNAs in the hippocampal tissue of rats after sevoflurane exposure. Among them, miR-130b-5p was found to be involved in the neuronal apoptosis pathway of acute spinal cord injury in both the rat ASCI model and the hypoxia cell model [29]. In addition, the putative target gene N-acetylglutamate synthase (Nags) catalyzes the transformation of L-glutamate to N-acetyl-L-glutamate (NAG), which is a specific cofactor for carbamoyl phosphate synthetase I in the urea cycle. Abnormal expression of Nags can lead to increased plasma ammonia levels and neurotoxicity [30]. It has been reported that Gonadotropin-Releasing Hormone (GnRH) is involved in central nervous system function and neurodegenerative issues, and exposure of neuron-like cells to GnRH can lead to enhanced estrogen levels. Moreover, other studies have demonstrated that GnRH increases the synthesis of 17 β -estradiol (E2) and overcomes cognitive decline caused by amyloid β (A β) neurotoxicity [31].

The hippocampus is known to be associated with cognitive function [32–34]. This study utilized the Morris Water Maze (MWM) test to assess cognitive behavior in neonatal rats at 8 weeks post-sevoflurane exposure, aiming to explore the impact of sevoflurane on long-term memory function. The sevoflurane group shown a notable increase in swimming latency and a significant decrease in crossing times during the MWM test [35,36]. Therefore, the study results suggest that dysregulated miRNAs and their interacting target mRNAs may play a critical role in the progression of hippocampal pathogenesis induced by sevoflurane exposure in neonatal rats and long-term cognitive impairment.

5. Conclusion

In summary, our present findings offer evidence of acute neuronal apoptosis and long-term behavioral impairment in the hippocampus of developing rats subsequent to relatively short-term exposure to sevoflurane. The study also revealed abnormal expression changes of miRNAs and mRNAs induced by sevoflurane exposure in neonatal rats, as well as detailed interaction networks displaying predicted pathways through miRNA-mRNA interactions associated with neurodegenerative phenotypes. However, limitations exist regarding the comparability of exposure durations between rats and humans. Past rodent studies on neurotoxicity typically employed exposure periods of less than 6 h. Therefore, due to various differences in relative anesthesia exposure duration and lifespan between rats and humans, we do not recommend overinterpreting our data directly into clinical practice in humans. Obtaining miRNA-mRNA profiles and target networks after sevoflurane exposure as a novel concept may have potential value in the study of anesthesia-induced developmental neurotoxicity.

Consent for publication

Not applicable.

Availability of data and material

The datasets used and/or analyzed in this investigation are accessible from the corresponding author upon request deemed reasonable.

Funding statement

This work was supported by Zhejiang Provincial Nature Science Foundation of China (LGF22H310002).

Data availability

The data that support the conclusions of this study can be obtained upon request from the corresponding author. Alternatively, they are available from the corresponding authors upon reasonable request.

CRedit authorship contribution statement

Yuanyuan Wang: Writing – original draft, Data curation. **Xin Men:** Methodology, Data curation. **Xiaodong Huang:** Validation. **Xiaoxiao Qiu:** Visualization. **Weilong Wang:** Software. **Jin Zhou:** Writing – review & editing. **Zhenfeng Zhou:** Writing – review & editing, Project administration, Funding acquisition.

Declaration of competing interest

The authors declare that they have no known competing financial interests or personal relationships that could have appeared to influence the work reported in this paper.

Acknowledgements

None.

Appendix A. Supplementary data

Supplementary data to this article can be found online at <https://doi.org/10.1016/j.heliyon.2024.e33333>.

References

- [1] S.C. Johnson, A. Pan, L. Li, M. Sedensky, P. Morgan, Neurotoxicity of anesthetics: mechanisms and meaning from mouse intervention studies, *Neurotoxicol. Teratol.* 71 (2019) 22–31.
- [2] D.C. Bellinger, J. Calderon, Neurotoxicity of general anesthetics in children: evidence and uncertainties, *Curr. Opin. Pediatr.* 31 (2) (2019) 267–273.
- [3] X. Liu, J. Ji, G.-Q. Zhao, General anesthesia affecting on developing brain: evidence from animal to clinical research, *J. Anesth.* 34 (5) (2020) 765–772.
- [4] C. Apai, R. Shah, K. Tran, S.H.A.H.S. Pandya, Anesthesia and the developing brain: a review of sevoflurane-induced neurotoxicity in pediatric populations, *Clin. Therapeut.* 43 (4) (2021) 762–778.
- [5] M. Sun, Z. Xie, J. Zhang, Y. Leng, Mechanistic insight into sevoflurane-associated developmental neurotoxicity, *Cell Biol. Toxicol.* 38 (6) (2022) 927–943.
- [6] M. Correia de Sousa, M. Gjorgjieva, D. Dolicka, C. Sobolewski, M. Foti, Deciphering miRNAs' action through miRNA editing, *Int. J. Mol. Sci.* 20 (24) (2019).
- [7] M. Tafrihi, E. Hasheminasab, miRNAs: biology, biogenesis, their web-based tools, and databases, *MicroRNA* 8 (1) (2019) 4–27.
- [8] S.P. Kabekkodu, V. Shukla, V.K. Varghese, D.S. J. S. Chakrabarty, K. Satyamoorthy, Clustered miRNAs and their role in biological functions and diseases, *Biol. Rev. Camb. Phil. Soc.* 93 (4) (2018) 1955–1986.
- [9] T.X. Lu, M.E. Rothenberg, MicroRNA, *J. Allergy Clin. Immunol.* 141 (4) (2018) 1202–1207.
- [10] K. Saliminejad, H.R. Khorram Khorshid, F.A.R.D.S. Soleymani, S.H. Ghaffari, An overview of microRNAs: biology, functions, therapeutics, and analysis methods, *J. Cell. Physiol.* 234 (5) (2019) 5451–5465.
- [11] S.K. Rashidi, A. Kalirad, S. Rafie, E. Behzad, M.A. Dezfouli, The role of microRNAs in neurobiology and pathophysiology of the hippocampus, *Front. Mol. Neurosci.* 16 (2023) 1226413.
- [12] D.C. Henshall, MicroRNA and epilepsy: profiling, functions and potential clinical applications, *Curr. Opin. Neurol.* 27 (2) (2014) 199–205.
- [13] S. Xu, R. Gao, L. Chen, Dexmedetomidine regulates sevoflurane-induced neurotoxicity through the miR-330-3p/ULK1 axis, *J. Biochem. Mol. Toxicol.* 35 (12) (2021) e22919.
- [14] X. Wei, S. Xu, L. Chen, LncRNA Neat1/miR-298-5p/Srpk1 contributes to sevoflurane-induced neurotoxicity, *Neurochem. Res.* 46 (2021) 3356–3364.
- [15] Y. Jiang, Y. Wang, Y. Sun, H. Jiang, Long non-coding RNA Peg 13 attenuates the sevoflurane toxicity against neural stem cells by sponging microRNA-128-3p to preserve Sox 13 expression, *PLoS One* 15 (12) (2020) e0243644.
- [16] L. Zhang, Q. Liu, Z. Xue, Y. Jia, H. Jiang, Sevoflurane regulating LncRNA Rik-203 contributes to neural differentiation via microRNA-4661-3p/BDNF pathway, *Res. Square* (2019) 1–18. <https://doi.org/10.21203/rs.2.288/v1>.
- [17] J.R. Lee, B. Joseph, R.D. Hofacer, B. Upton, S.Y. Lee, L. Ewing, B. Zhang, S.C. Danzer, A.W. Loepke, Effect of dexmedetomidine on sevoflurane-induced neurodegeneration in neonatal rats, *Br. J. Anaesth.* 126 (5) (2021) 1009–1021.
- [18] S. Tam, M.-S. Tsao, J.D. Mcpherson, Optimization of miRNA-seq data preprocessing, *Briefings Bioinf.* 16 (6) (2015) 950–963.
- [19] M. Pertea, D. Kim, G.M. Pertea, J.T. Leek, S.L. Salzberg, Transcript-level expression analysis of RNA-seq experiments with HISAT, StringTie and Ballgown, *Nat. Protoc.* 11 (9) (2016) 1650–1667.
- [20] A.J. Davidson, Anesthesia and neurotoxicity to the developing brain: the clinical relevance, *Pediatric Anesthesia* 21 (7) (2011) 716–721.
- [21] Y. Tian, K.-Y. Chen, L.-D. Liu, Y.-X. Dong, P. Zhao, S.-B. Guo, Sevoflurane exacerbates cognitive impairment induced by $\alpha 1-40$ in rats through initiating neurotoxicity, neuroinflammation, and neuronal apoptosis in rat Hippocampus, *Mediat. Inflamm.* (2018) 2018.
- [22] M.S. Hipp, P. Kasturi, F.U. Hartl, The proteostasis network and its decline in ageing, *Nat. Rev. Mol. Cell Biol.* 20 (7) (2019) 421–435.
- [23] X. Kang, X. Li, Y. Li, Sevoflurane suppresses the proliferation, migration and invasion of colorectal cancer through regulating Circ_0000423/miR-525-5p/SGP11 network, *Cell. Mol. Bioeng.* 15 (2) (2022) 219–230.
- [24] S. Zheng, L. An, X. Cheng, Y. Wang, Sevoflurane causes neuronal apoptosis and adaptability changes of neonatal rats, *Acta Anaesthesiol. Scand.* 57 (9) (2013) 1167–1174.
- [25] Z. Pan, X.-F. Lu, C. Shao, C. Zhang, J. Yang, T. Ma, L.-C. Zhang, J.-L. Cao, The effects of sevoflurane anesthesia on rat hippocampus: a genomic expression analysis, *Brain Res.* 1381 (2011) 124–133.
- [26] F. Liu, B. Gong, Q. Gu, S. Liu, C.M. Fogle, T.A. Patterson, J.P. Hanig, J.R.W. Slikker, C. Wang, Application of microRNA profiling to understand sevoflurane-induced adverse effects on developing monkey brain, *Neurotoxicology* 81 (2020) 172–179.
- [27] R. Minz, P.K. Sharma, A. Negi, K.K. Kesari, MicroRNAs-based theranostics against anesthetic-induced neurotoxicity, *Pharmaceutics* 15 (7) (2023) 1833.
- [28] C. Apai, R. Shah, K. Tran, S.P. Shah, Anesthesia and the developing brain: a review of sevoflurane-induced neurotoxicity in pediatric populations, *Clin. Therapeut.* 43 (4) (2021) 762–778.
- [29] H. Zhang, D. Li, Y. Zhang, J. Li, S. Ma, J. Zhang, Y. Xiong, W. Wang, N. Li, L. Xia, Knockdown of lncRNA BDNF-AS suppresses neuronal cell apoptosis via downregulating miR-130b-5p target gene PRDM5 in acute spinal cord injury, *RNA Biol.* 15 (8) (2018) 1071–1080.
- [30] G. Zhao, Z. Jin, N.M. Allowell, M. Tuchman, D. Shi, Crystal structure of the N-acetyltransferase domain of human N-acetyl-L-glutamate synthase in complex with N-acetyl-L-glutamate provides insights into its catalytic and regulatory mechanisms, *PLoS One* 8 (7) (2013) e70369.
- [31] K. Skrapits, M. Sárvári, I. Farkas, B. Göcz, S. Takács, É. Rumlper, V. Vácsi, C. Vastagh, G. Rác, A. Matolcsy, The cryptic gonadotropin-releasing hormone neuronal system of human basal ganglia, *Elife* 10 (2021) e67714.
- [32] H. Eichenbaum, Hippocampus: cognitive processes and neural representations that underlie declarative memory, *Neuron* 44 (1) (2004) 109–120.
- [33] T.E. Evans, H.H. Adams, S. Licher, F.J. Wolters, A. van der Lugt, M.K. Ikram, M.J. O'Sullivan, M.W. Vernooij, M.A. Ikram, Subregional volumes of the hippocampus in relation to cognitive function and risk of dementia, *Neuroimage* 178 (2018) 129–135.
- [34] Y. Wan, J. Xu, D. Ma, Y. Zeng, M. Cibelli, M. Maze, Postoperative impairment of cognitive function in rats: a possible role for cytokine-mediated inflammation in the hippocampus, *The Journal of the American Society of Anesthesiologists* 106 (3) (2007) 436–443.
- [35] R. Gerlai, Behavioral tests of hippocampal function: simple paradigms complex problems, *Behav. Brain Res.* 125 (1–2) (2001) 269–277.
- [36] L. Mo, Z. Yang, A. Zhang, X. Li, The repair of the injured adult rat hippocampus with NT-3-chitosan carriers, *Biomaterials* 31 (8) (2010) 2184–2192.